Original Research Article

Green synthesis and characterization of silver nanoparticles using combretum micranthum leaves extract as bio reductor

Tongonmanegde Léonard Ouédraogo*, Sidiki Zongo, Moussa Sougoti, Sié Zacharie Kam, Fabrice Bado, Jean Koulidiati, Antoine Béré

Laboratory of Physics and Chemistry of Environment, Department of Physics, Université Joseph Ki-Zerbo, 03 BP 7021, Ouagadougou, Burkina Faso

ARTICLE INFORMATION

ABSTRACT

In this work, silver nanoparticles were synthesized from silver nitrate using combretum micranthum leaves extract as a reducing and capping agent. The optical characterization through UV visible spectroscopy revelated a characteristic peak of surface plasmon resonance at 425 nm, while the particle size calculations based on the Mie diffusion theory indicated sizes ranging from 32.5 nm to 44.5 nm. The effects of different reaction parameters including the initial concentration of the precursor and the percentage of the leaves extract, were analyzed. The optimal conditions for the synthesis at room temperature are 0.5 g/L and 7.5 mM, respectively, for the plant extract's weight concentration and the precursor's initial concentration.

Graphical Abstract
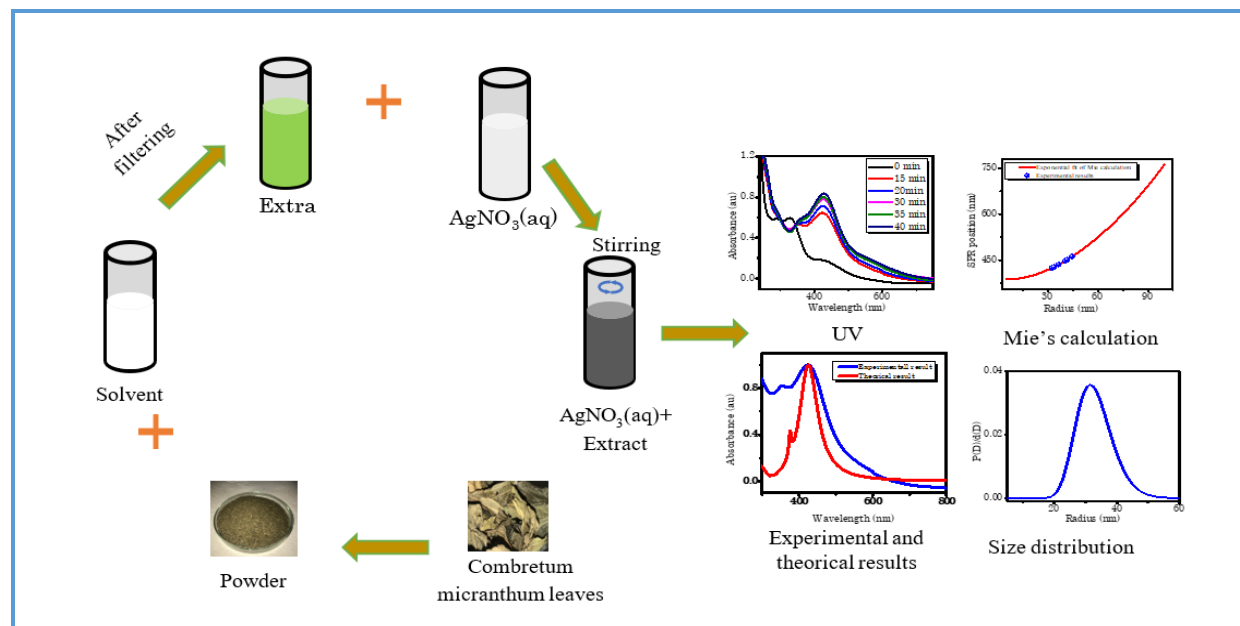
Introduction

Nanoparticles have recently attracted considerable interest due to their multifunctional properties and promising applications in various fields including catalysis, optics, and defense [1–3]. In recent years, metallic nanoparticles, particularly silver nanoparticles, have unbeatable physicochemical and biological properties such as electrical conductivity, catalytic, biological, and antimicrobial activity [4]. One of the most important areas of nanotechnology is the synthesis of different nanoparticles such as silver, gold, and iron. In general, nanoparticles are synthesized using various physical, chemical, and biological methods that are quite costly, and potentially harmful to the environment. In addition, these methods generally have some drawbacks such as dangerous and challenging reaction conditions, tedious preparation, long reaction times, high temperatures, low yields, expensive capping agents, use of organic solvents leading to environmental pollution and high energy consumption [5]. Thus, given the current environmental and economic concerns, the green synthesis of nanoparticles based on plant extracts has become a suitable alternative to physical and chemical methods. The use of plant extracts and other natural resources for the green synthesis of nanoparticles has proven to be an excellent method as it does not use toxic chemicals. It has many advantages, including environmental friendliness and suitability for pharmaceutical and biomedical applications [6, 7]. For the synthesis of silver nanoparticles, the literature reports different plants such as Eichornia crassipes [8], the skin of Citrus sinensis [9], the extract of the roots of carissa carandas [10], leaves and barks of Ocimum basilicum [11], flowers of the parasitic plant Cascuta reflexa [12], plant residues of Artocarpus altilis [13], flowers of Spartium junceum [14], seeds of Xanthium strumarium [15], and leaves of celosia argentea [16]. In the present work, the plant of combretum micranthum was used for the green synthesis of silver nanoparticles because of its availability, antioxidant properties and its numerous

virtues, especially for the treatment of some diseases such as diabetes, diarrhea, hepatitis, jaundice [17, 18]. It is a plant of the herbaceous family, widespread in the Sudano-Sahelian regions of West Africa. Previous phytochemical studies have indicated that extracts from the leaves of the combretum micranthum plant contain flavonoids, including vitexin, isovitexin, orientin, ommoorientin, myricetin-O-rutinoside; alkoloids, including stachydrin, hydroxyl-stachydrin, and choline; sugar alcohols, including m-inositol and sorbitol; and flavanic alkaloids, including kinkeloid A, B, C, and D [19]. The silver nanoparticles were synthesized using a green, fast and easy method using combretum micranthum leaf extract which acts as a reducing and capping agent reducing the silver ion into silver nanoparticles. In addition, the effect of some reaction parameters such as interaction time, extract rate in the reaction medium and the initial concentration of the precursor was studied. These ecologically synthesized nanoparticles were evaluated using UV-visible spectroscopy and by a numerical calculation based on Mie theory.

Materials and Methods

Bioactive components extraction

Decoction and maceration techniques are the most commonly used conventional extraction methods due to their effectiveness and scope. Temperature is the main difference between them. Some thermally unstable bioactive components are destroyed at high temperatures applied during decoction, so milder temperature through gentle maceration would be better [20]. Modern extraction methods, such as microwave-assisted extraction [21], ultrahigh-pressure extraction [22], and supercritical carbon dioxide extraction [23], have various advantages such as reduced extraction time and low extraction temperature, simple maceration, more convenient, and less expensive in terms of instrumentation. Dry leaves of combretum micranthum were purchased at the market de Ouagadougou, Burkina Faso, without particular treatment. 2 g of the grounded leaves were hydrated in 200 mL of distilled water at room temperature for 2 h. The extracted dye was thereafter filtered and used for the synthesis of silver nanoparticles. The silver nitrate was supplied from Sigma-Aldrich.

Synthesis process of silver nanoparticles

The synthesis process of nanoparticles was as follows: 5 mL of the extract of combretum micranthum leaves was added to 95 mL of the aqueous solution of silver nitrate in a 200 mL flask. The reaction medium was put under continuous stirring at room temperature for 4 h. Figures 1 and 2 demonstrate the synthesis process and the mechanism of green synthesis of silver nanoparticles, respectively.
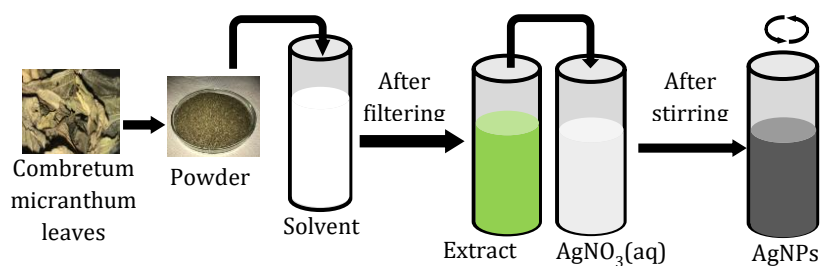

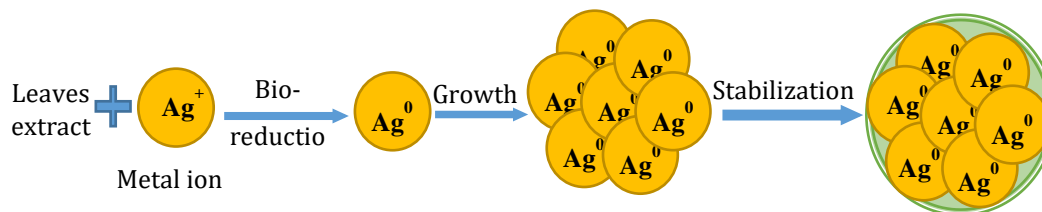**Figure 1.** Schematic illustration of the synthetic steps of AgNPs

Figure 2. Mechanism of silver nanoparticle green synthesis process.

Characterization

The dual-beam UV-visible spectrophotometer (HITACHI, model U2000) with a spectral band ranging from 190 nm to 1100 nm was used to record the UV spectra for optical properties. The determination of the size of the nanoparticles was carried out using Mie calculations which describe the diffusion of light by aggregates of matter whose refractive index differs from that of its environment. The model is based on the solution of Maxwell's equations in spherical coordinates using the expansion of magnetic and electric fields and taking into account the discontinuity of the dielectric constant between the sphere and the surrounding medium [24]. These solutions describe the scattering, extinction, and absorption of the electromagnetic wave as a function of two parameters m and x [24–26] are given in Equations 1, 2, and 3:

$$Q_{sca} = \frac{2}{x^2} \sum_{n=1}^{\infty} (2l+1)\left(|a_n|^2 + |b_n|^2\right) \qquad (1)$$

$$Q_{ext} = \frac{2}{x^2} \sum_{n=1}^{\infty} (2l+1)\operatorname{Re}\{a_n + b_n\} \qquad (2)$$

$$Q_{abs} = Q_{ext} - Q_{sca} \qquad (3)$$

a_n and b_n are Mie coefficients given by the equations 4 and 5.

$$a_n = \frac{\psi_n(x)\psi_n'(mx) - m\psi_n'(x)\psi_n(mx)}{\zeta_n(x)\psi_n'(mx) - m\xi_n'(x)\psi_n(mx)} \qquad (4)$$

$$b_n = \frac{m\psi_n(x)\psi_n'(mx) - \psi_n'(x)\psi_n(mx)}{m\zeta_n(x)\psi_n'(mx) - \xi_n'(x)\psi_n(mx)} \qquad (5)$$

ψ_l and ζ_n are Riccati-Bessel and Riccati-Hankel function respectively, the prime denotes the first order derivate. x a size parameter of the nanoparticle and m is its normalized refractive index.

Results and Discussion

UV-visible absorption

When the extract of combretum micranthum leaves was added to the silver nitrate solution, a rapid change in color of the mixture was observed, indicating a reduction of ions silver to metal silver [27] by the active molecules of combretum micranthum leaves [19]. The formation of silver nanoparticles was high-lighted by a UV-visible spectrophotometer. Indeed, noble metal nanoparticles possess unique optical properties due to the collective oscillation of conduction electrons: The surface plasmon resonance (SPR), whose peak and absorption band depends on the shape and the size distribution of the nanoparticles [26]. Figure 3 reveals the absorption spectra as a function of time, of the nanoparticles. The absorption maximum due to the SPR was observed at 425 nm, convenient to the formation of silver nanoparticles. The Figure 4 shows an increase in the intensity of the absorption peak over time, indicating an enhancement of the formation of silver nanoparticles without variation in the wavelength of the SPR peak. This wavelength stabilization of the SPR peak indicates that the nanoparticles do not aggregate.
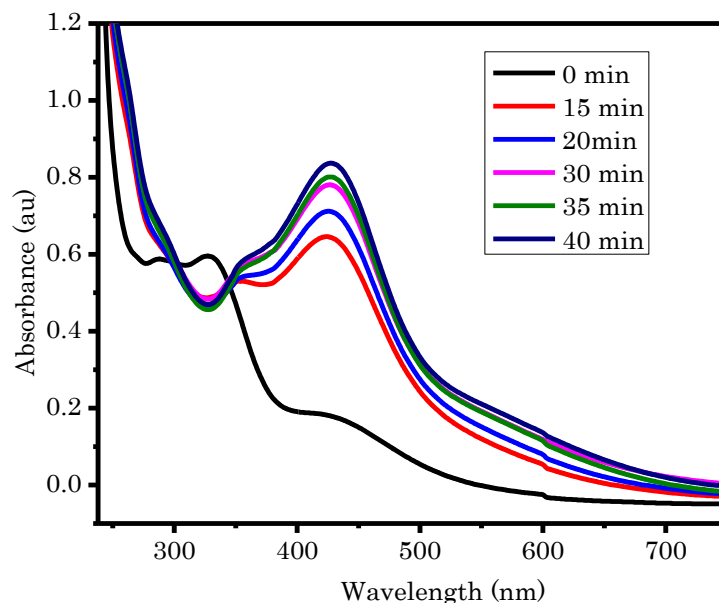
Figure 3. UV-visible absorption spectrum of silver nanoparticles
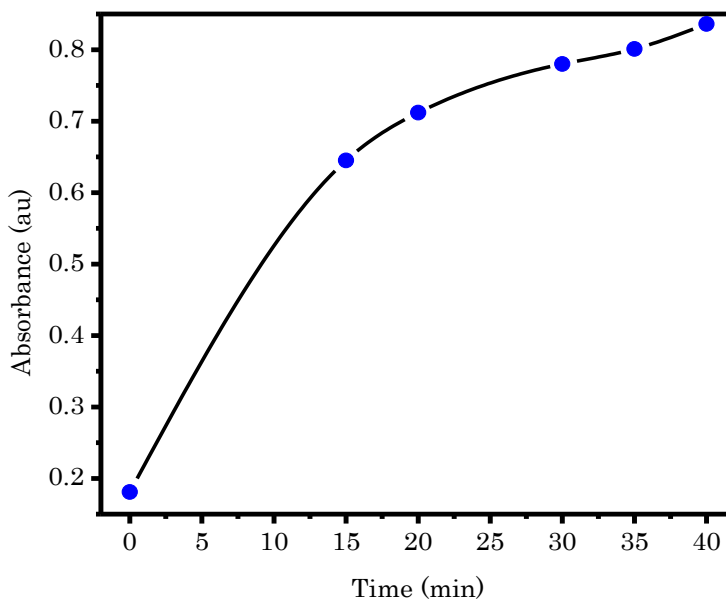

Figure 4. The intensity of the SPR as a function of reaction time

The influence of the amount of plant extract on the formation of nanoparticles was studied. Figure 5 demonstrates the absorbance intensity spectrum obtained at different concentrations of leaves extract. An increase in the absorption peak's intensity is observed as the concentration of the leaves extract. This shows that the reduction rate of the metal ions increases with the percentage of leaves extract. However, as shown in Figure 6, there is a relatively more significant shift in the position of the SPR peak over time as the concentration

of extract increases. This shift is due to the excessive number of biomolecules present at high extract concentrations that initiate a secondary reduction process on the surface of the nuclei, increasing the particle size. These experimental results revealed that the optimum extract concentration was 5 g/L for the synthesis of silver nanoparticles.

The effect of initial precursor concentration was evaluated. The formation of silver nanoparticles occurs in two steps; the first step is the formation of nuclei and the second is the growth in size. Thus, it is necessary to optimize the initial concentration of the precursor so that the nuclei form faster and grow more slowly [28]. Figure 7 shows that the SPR peak wavelength depends on the precursor's initial concentration. The SPR wavelength decreased from 440 nm to 425 nm when the concentration varied from 5.5 mM to 7.5 mM and then increased beyond this concentration. This increase in the concentration of the precursor results in increasing the number of silver nuclei, and consequently making the particles smaller. However, an excessive number of nuclei will be generated at high precursor concentrations, which leads to nuclei agglomeration and particle size growth [28, 29].
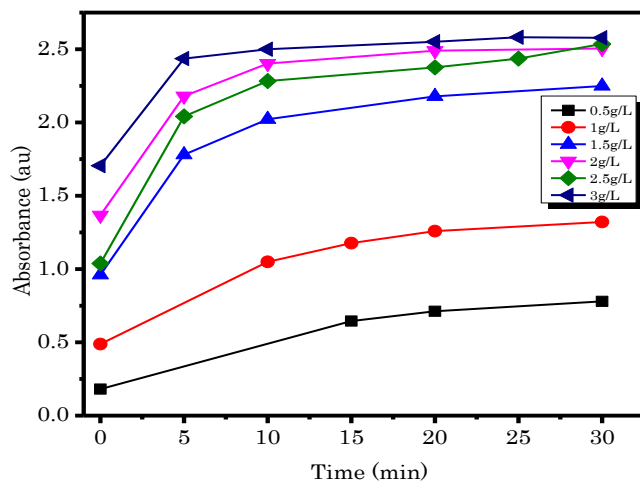

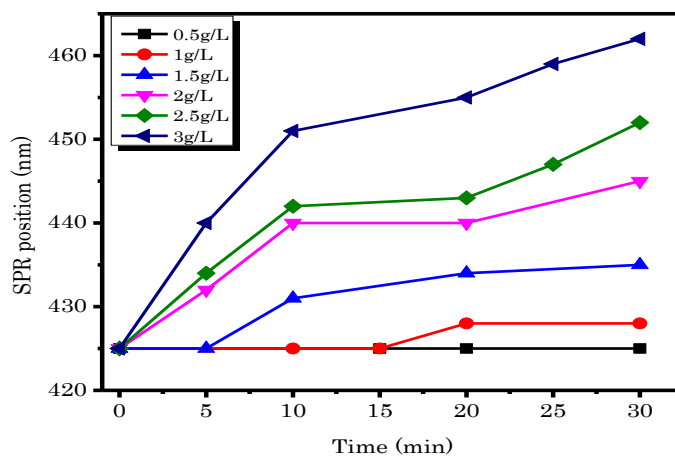**Figure 5.** Effect of the amount of extract on the reduction rate

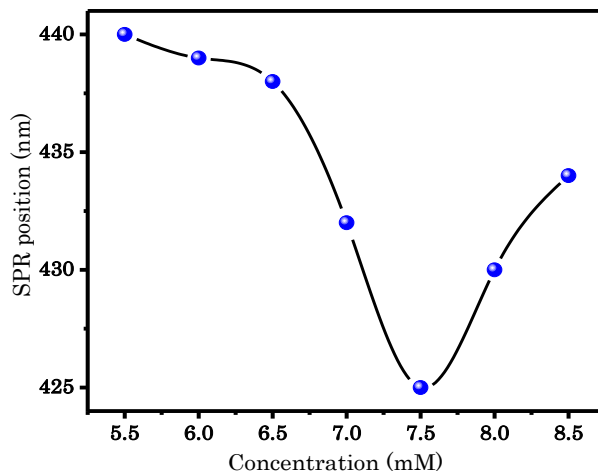**Figure 6.** Effect of the extract rate on the SPR peak position

Figure 7. Effects of the initial precursor concentration on the wavelength of the SPR peak

Theorical estimation of particles size

To obtain the approximate size of the nanoparticles, it was necessary to refer to the calibration curve presented in Figure 8, obtained by a numerical simulation of Mie equations by changing the radius of the nanoparticle from 5 nm to 100 nm with an interval of 5 nm. As seen in Figure 8, wavelength evolution of the SPR peak occurred when the size of the nanoparticle increased, which was resulted from the change of the mean free path of the electrons [30]. The SPR peak is increasing exponentially. This was determined by fitting the theoretical data with an exponential function presented in Equation 6 with $R^2 = 99.96\%$.

$$\lambda_{SPR}(r) = 1089\exp(-0.03388r) + 2815\exp(0.009364r)$$
(6)

Figure 9 reveals that the synthesized particles' radius for the different concentrations varies from 32.5 nm to 44.5 nm.
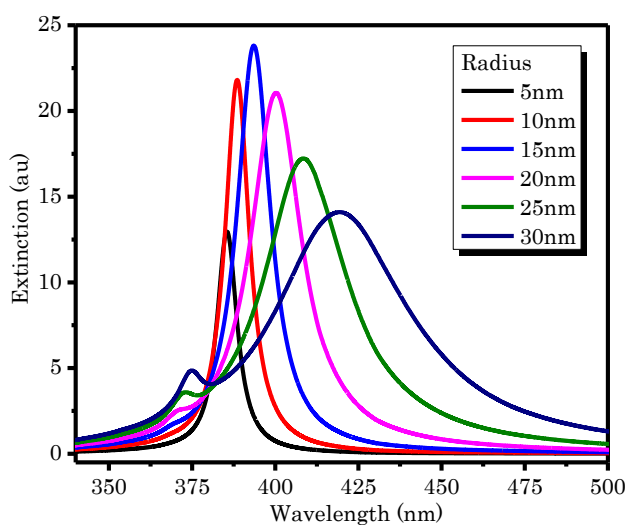

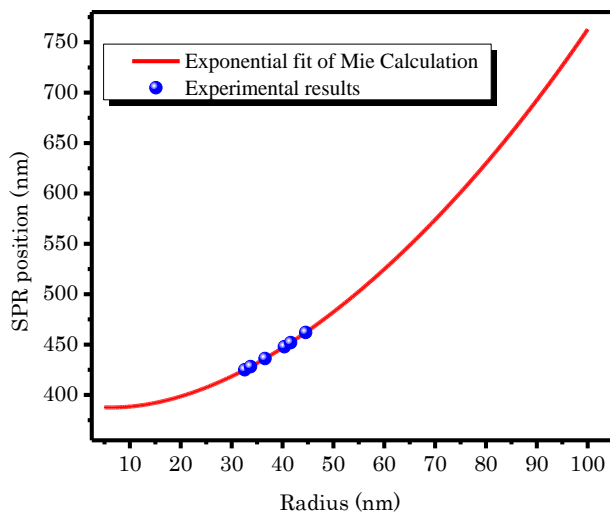**Figure 8.** Theorical absorption spectrum of silver nanoparticles calculating using Mie theory

Figure 9. Approximation of silver nanoparticle size using Mie theory

Statistical analysis

Under optimal conditions, a better agreement was observed between the theoretical and experimental results when the particle's radius was 32.5 nm. The normalized absorption spectra (theoretical and experimental) are presented in Figure 10. Polydisperse nanoparticle systems obey a log-normal size distribution [31, 32]. Thus, the UV visible absorption spectra are fitted using the log-normal function shown in Equation 7 to obtain the standard deviation.

$$P(D)/dD = \frac{1}{\sqrt{2\pi}\sigma D} \exp\left(-\frac{\ln^2(D/D_0)}{2\sigma^2} \right) \qquad (7)$$

The standard deviation and the average particle size obtained from Mie's theory are used to generate the nanoparticle size distribution, as shown in Figure 11. In addition, the particles are dispersed as follows: 68% have a radius between 27.7 nm and 38.05 nm, and 98% have a radius between 23.74 nm and 44.8 nm.
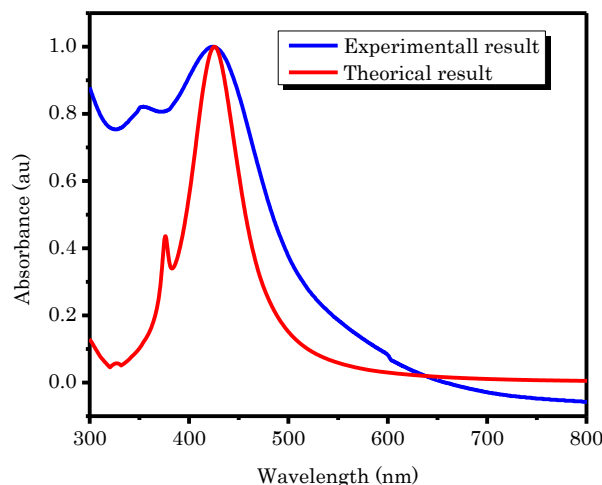

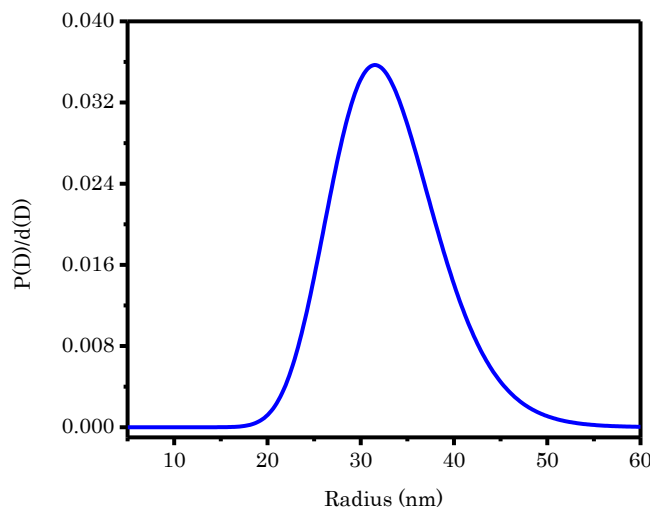**Figure 10.** Comparison of experimental and theoretical results

Figure 11. Lognormal size distribution

Conclusions

In this work, we presented the green synthesis of silver nanoparticles using the extract of the leaves of the plant combretum micranthum, a species with therapeutic properties, both as a reducing agent of metal ions and stabilizer of silver nanoparticles. Green synthesis is a technique capable of producing silver nanoparticles at room temperature that is -effective, environmentally friendly, does not involve harmful and toxic chemicals, and is therefore environmentally acceptable. The synthesized silver nanoparticles were characterized using UV-visible spectroscopy. Different reaction conditions were analyzed, and under optimal conditions, the absorption spectra revealed a peak at 425 nm corresponding to the surface plasmon resonance of the synthesized silver nanoparticles. Moreover, a numerical calculation based on Mie theory revealed that the obtained particles have an average radius of 32.5 nm. This technique is potentially interesting and promising for synthesizing other metallic nanoparticles for medical applications.

Disclosure Statement

No potential conflict of interest was reported by the authors.

Authors' contributions

All authors contributed to data analysis, drafting, and revising of the paper and agreed to be responsible for all the aspects of this work.

References

[1]. Qi L., Zhang K., Qin W., Hu Y. *Chem. Eng. J.*, 2020, **388**:124252 [Crossref], [Google Scholar], [Publisher]

[2]. Ferreira D.P., Costa S.M., Felgueiras H.P., Fangueiro R. *Key Eng. Mater.*, 2019, **812**:66 [Crossref], [Google Scholar], [Publisher]

[3]. Mohamed Fahmy H., Mahmoud Mosleh A., Abd Elghany A., Shams-Eldin E., Samy Abu Serea E., Ashour Alia S., Shalan A.E. *RSC Adv.*, 2019, **35**:20118 [Crossref], [Google Scholar], [Publisher]

[4]. Nanaei M., Nasseri M.A., Allahresani A., Kazemnejadi M. *SN Appl. Sci.*, 2019, **8**:1 [Crossref], [Google Scholar], [Publisher]

[5]. Arshadi E., Sedaghat S., Moradi O. *Asian J. Green Chem.*, 2018, **3**:41 [Crossref], [Publisher]

[6]. Mousavi S.M., Hashemi S.A., Ghasemi Y., Atapour A., Mohammad Amani A., Savar Dashtaki A., Babapoor A., Arjmand O. *Artif. Cells, Nanomedicine Biotechnol.*, 2018, **46**:855 [Crossref], [Google Scholar], [Publisher]

[7]. Owaid M.N. Ayesh Rabeea M., Aziz A., S.Jameel M., Dheyab M.A. *Environ. Nanotechnology, Monit. Manag.*, 2019, **12**:100270 [Crossref], [Google Scholar], [Publisher]

[8]. Jayasree D., Sreebamol K.S., Gopinath A. *Asian J. Green Chem.*, 2022, **6**:14 [Crossref], [Publisher]

[9]. Nahar K., Rahaman M.H., Khan G.M.A., Islam M.K., Al-Reza S.M. *Asian J. Green Chem.*, 2021, **5**:135 [Crossref], [Google Scholar], [Publisher]

[10]. Manjare S.B., Sharma S.G., Gurav V.L., Kunde M.R., Patil S.S., Thopate S.R. *Asian J. Nanosci. Mater.*, 2020, **3**:58 [Crossref], [Google Scholar], [Publisher]

[11]. Elumalai D., Sathiyaraj M., Vimalkumar E., Kunyl Kaleena P., Hemavathi M., Venkatesh P. *Asian J. Green Chem.*, 2019, **3**:103 [Crossref], [Google Scholar], [Publisher]

[12]. Shaikh N.S., Shaikh R.S., Kashid S. *Asian J. Nanosci. Mater.*, 2020, **3**:121 [Crossref], [Google Scholar], [Publisher]

[13]. Nayagam V., Palanisamy K., Thiraviadoss D. *Asian J. Nanosci. Mater.*, 2019, **2**:301 [Crossref], [Google Scholar], [Publisher]

[14]. Nasseri M.A., Shahabi M., Allahresani A., Kazemnejadi M. *Asian J. Green Chem.*, 2019, **3**:382 [Crossref], [Google Scholar], [Publisher]

[15]. Shaikh R., Nayab J., Shaikh N. *Asian J. Green Chem.*, 2021, **5**:313 [Crossref], [Google Scholar], [Publisher]

[16]. Raghavan S., Siddique J.F., Anbalagan N., Kirthi V. *Asian J. Nanosci. Mater.*, 2020, **3**:251 [Crossref], [Google Scholar], [Publisher]

[17]. Seck S.M. Doupa D., Guéye Dia D., Assane Diop E., Ardiet D.L., Campos Nogueira R., Graz B., Diouf B. *J. Hum. Hypertens.*, 2017, **32**:75 [Crossref], [Google Scholar], [Publisher]

[18]. Zahoui O.S., Soro T.Y., Yao K.M., Nene-Bi S.A., Traoré F. *Phytotherapie*, 2017, **15**:138 [Crossref], [Google Scholar], [Publisher]

[19]. Welch C., Zhen J., Bassène E., Raskin I., Simon J.E., Wu Q. *J. Food Drug Anal.*, 2018, **26**:487 [Crossref], [Google Scholar], [Publisher]

[20]. Paranjpe S.S., Ferruzzi M., Morgan M.T. *LWT-Food Sci. Technol.*, 2012, **48**:147 [Crossref], [Google Scholar], [Publisher]

[21]. Dhobi M., Mandal V., Hemalatha S. *J. Chem. Metrl.*, 2009, **3**:13 [Google Scholar], [Publisher]

[22]. Sami S., Ashraf B., Maria Gretel Michel B., Alain D., Zouhair T., Yves D. *Food Anal. Methods*, 2020, **13**:1556 [Crossref], [Google Scholar], [Publisher]

[23]. Essien S.O., Young B., Baroutian S. *Trends Food Sci. Technol.*, 2020, **97**:156 [Crossref], [Google Scholar], [Publisher]

[24]. Pinchuk A.O., Schatz G.C., *Mater. Sci. Eng. B*, 2008, **149**:251 [Crossref], [Google Scholar], [Publisher]

[25]. Quinten M., Optical Properties of Nanoparticle Systems; Wiley-VCH; Allemande; 2011; p123 [Crossref], [Publisher]

[26]. Lahamani M., Bréchignac C., Houdy P. Les nanosciences-Nanomatériaux et Nanochimie; Edition Be.; Paris, 2006; p 205

[27]. Balan K., Qing W., Wang Y., Liu X., Palvannan T., Wang Y., Maa F., Zhang Y. *RSC*

Adv., 2016, **6**:40162 [Crossref], [Google Scholar], [Publisher]

[28]. Nagar N., Devra V. *Mater. Chem. Phys.*, 2018. [Crossref], [Google Scholar], [Publisher]

[29]. Vanaja M., Paulkumar K., Baburaja M., RajeshkumarS., Gnanajobitha G., Malarkodi C., Sivakavinesan M., Annadurai G. *Bioinorg. Chem. Appl.*, 2014, **2014**:8 pages [Crossref], [Google Scholar], [Publisher]

[30]. Jonathan P., Sébastien Z., Geoffroy C., Corintin B., Yannis C. *Union des professeurs Phys. Chim.*, 2016, **110**:1339 [Google Scholar], [Publisher]

[31]. Mankad V., Kumar R.K., Jha P.K. *Nanosci. Nanotechnol. Lett.*, 2013, **5**:889 [Crossref], [Google Scholar], [Publisher]

[32]. Desai R., Mankad V., Gupta S.K., Jha P.K. *Nanosci. Nanotechnol. Lett.*, 2012, **4**:30 [Crossref], [Google Scholar], [Publisher]